Study Of The Mechanical Behavior Of Elastomer Protective Materials

Lotfi Harrabi, Tarek Abboud, Toan Vu-Khanh, Patricia Dolez, Jaime Lara

Abstract: In order to study the mechanical behaviour of elastomers at large deformations, a theoretical description was developed for the loading-unloading hysteresis loop at large deformations and as a function of the strain rate. Bergström and Boyce's proposition that the elastomer behaviour is controlled by two contributions, the first one corresponding to the equilibrium state and the second one to a non-linear rate-dependent deviation from that equilibrium state, and their use of Zener's rheological model, were applied to an uniaxial tension configuration. A validation of the description was performed with nitrile rubber. A good agreement of the theoretical description with experimental results was obtained. This simple description of the hysteresis behaviour of elastomers as a function of the strain rate provides a useful tool for estimating the mechanical behaviour at various strain rates, with potential application in the design of protective gloves.

Index Terms: elastomer, Nitrile rubber, hysteresis, large deformation, variable strain rate.

1 INTRODUCTION

The use of protective gloves at the workplace allows a reduction in injury occurrence and seriousness. However, wearing protective gloves may also cause a decrease in the ability to perform tasks and an increased level of muscular fatigue, for example due to their lack of suppleness [1]. Ultimately, this can either lead to resistance to wearing the needed protective gloves, with an increase in direct injuries like skin laceration, or to the occurrence of indirect and more long-term injuries like tendonitis. The design of gloves with adequate properties requires knowledge of the constitutive material mechanical behaviour. While some studies have reported on the development of methods for the characterization of protective glove stiffness, either mechanical [2, 3] or with human subjects [3, 4], as well as on the effect of these properties on task performance [5], not much has been done on the dynamic mechanical behaviour of gloves. Yet, deformations subjected to gloves in use may involve a wide range of strain rates. This question is particularly relevant in the case of viscoelastic compounds like elastomers, which constitute a choice material for protective gloves due to their good flexibility and elasticity as well as their resistance to a number of hazards [6]. For example, nitrile rubber offers good chemical performance [7, 8]. In the work reported in this paper, the dynamic mechanical behaviour of elastomers is studied at conditions relevant to the use of protective gloves, i.e. at large deformation and variable strain rates, through the analysis of the hysteresis loop corresponding to a loading-unloading cycle. Several authors have worked on the mechanical behaviour of elastomers [9-30]. Two approaches can be identified: the molecular approach is based on network physics [12-14, 21, 22, 27, 31] while the phenomenological approach relies on mathematical considerations [7, 9-11, 15, 24, 25, 32].

- *Lotfi Harrabi, Tarek Abboud, Toan Vu-Khanh, Patricia Dolez, Jaime Lara*
- *École de Technologie Supérieure (ÉTS), 1100, Notre-Dame West, Montréal (Québec) H3C 1K3; Dr Lotfi Harrabi is the corresponding author for this paper : lotfi.harrabi.1@ens.etsmtl.ca*
- *Institut de recherche Robert-Sauvé en santé et en sécurité du travail, 505 boul. de Maisonneuve Ouest, Montréal. Canada H3A 3C2*

For example Mooney and Rivlin have lay the basis for large deformation theories for elastic materials. More recently, Arruda and Boyce have proposed a new description known as the eigth chain model, which is derived from non-Gaussian statistics theory [31]. It has been used successfully to predict the behaviour of elastomers up to failure. In particular, it has had applications in optics [33] and structural mechanics [20]. In the case of cyclic loading, even if they are highly elastic, elastomers display different paths for loading and unloading [12, 34]. This hysteresis loop corresponds to the energy dissipated during the loading-unloading process. After a few cycles, this loop tends to stabilise as shown by Mullins [35]. Even if time is a fundamental factor to consider when dealing with viscoelastic materials like elastomers, very few people have looked at the effect of strain rate on the mechanical behaviour of elastomers, and in particular on the hysteresis loop. Some have limited their study to the effect of strain and stress amplitude on the hysteresis loss [36]. Others have looked at the effect of the strain rate on the parameters of the model used for finite element analysis [37]. Bergström and Boyce were the first ones to consider the case with attention; they studied the effect of strain rate on the hysteresis loop of elastomers when working in compression and at large deformation [38]. They proposed a theoretical description based on the three-element Zener rheological model and the use of non-linear constants. The same principle was later applied to the case of thermoplastics for example [39]. Bergström and Boyce's idea consists in decomposing the hysteresis loop in two parts, one characterizing the equilibrium state of the deformed elastomer, and the other a time-dependant deviation from that equilibrium [38]. The resulting total stress combines an elastic contribution and a time-dependent one. As an alternative to Bergström and Boyce's 3D complex tensorial description relative to compression, this paper proposes a simplified model based on the same principles but corresponding to a unidirectional treatment of tensile deformation. It is validated by comparison with experimental tests performed with nitrile rubber samples.

2 EXPERIMENTAL METHOD

The studied material is nitrile rubber. Samples were cut from protective gloves (Best Glove manufacturing, model number 412, thickness 0.6 mm) using dye C of the ASTM D 412 standard test method for measuring the tensile properties of elastomers [40]. The tests were performed with a MTS mechanical test frame, model Alliance RF/200 using a 1000 N

load cell. For each condition, a minimum of three replicates were measured. Maximum loading and loading-unloading experiments were carried out at various loading rates. Figure 1 illustrates the loading-unloading sequence applied in the case of a 50 mm/min loading rate.

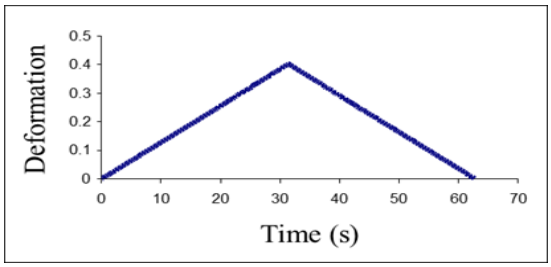

(a) Deformation

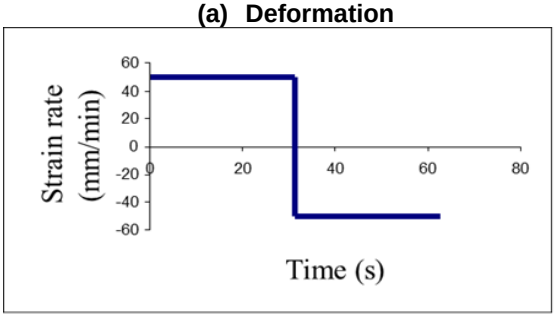

(b) Strain rate

Figure 1: *Loading-unloading test (strain rate 50 mm/min)*

3 THEORETICAL MODEL

A combination of a non linear viscoelastic model and Zener standard rheological description of solids (see Figure 2) has been used to predict the hysteresis behavior of nitrile rubber at large deformations and at different strain rates. More specifically, it is proposed that the hysteresis behavior of the elastomer membrane is due to the contribution of two parts: the first one (A) corresponds to the equilibrium state and can be represented by a spring R_1 while the second one (B) is due to the deviation from this equilibrium and is described by a spring R_2 in series with a damper. To take into account the non linear behavior of nitrile rubber, both springs are described using the Arruda-Boyce eight-chain model [31], while a simple linear function of the strain rate logarithm is used for the damper v

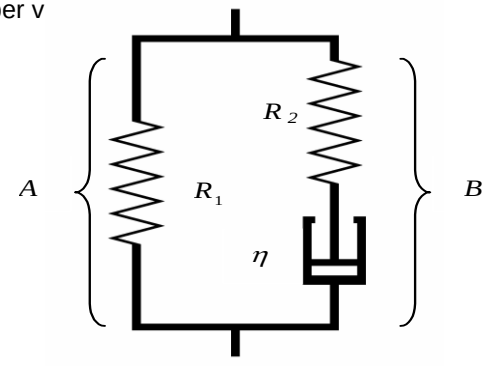

Figure 2: *Schematic representation of the Zener viscoelastic model*

The differential equation corresponding to Zener's three-element model is provided by Equation (1).

$$\dot{\sigma} + \frac{E^{(R_2)}}{\eta}\sigma = (E^{(R_1)} + E^{(R_2)})\dot{\varepsilon} + \frac{E^{(R_1)}E^{(R_2)}}{\eta}\varepsilon \quad (1)$$

Where $E^{(R_1)}$ is the modulus of spring R_1, $E^{(R_2)}$ is the modulus of spring R_2 and η is the viscosity of the damper, σ is the stress, $\dot{\sigma}$ is the variation of the stress with time, ε is the strain and $\dot{\varepsilon}$ is the strain rate. Equation (2) represents the solution of Equation (1) in terms of time variation of the stress for a loading-unloading cycle.

$$\sigma(t) = \zeta \begin{cases} \left[\eta + E^{(R_1)}t - \eta\, e^{-\frac{E^{(R_2)}}{\eta}t}\right] - \\ 2\left[\eta + E^{(R_1)}(t-\tau_{1/2}) - \eta\, e^{-\frac{E^{(R_2)}}{\eta}(t-\tau_{1/2})}\right] H(t-\tau_{1/2}) \end{cases} \quad (2)$$

With t is the time, ζ is the strain rate, $\tau_{1/2}$ is the half cycle time and H is the Heaviside function defined by Equation (3).

$$\begin{cases} H(t-\tau_{1/2}) = 0 \quad pour \quad t \le \tau_{1/2} \\ H(t-\tau_{1/2}) = 1 \quad pour \quad t \ge \tau_{1/2} \end{cases} \quad (3)$$

3.1 Representation of the equilibrium state

The strain-stress relationship corresponding to the part A of the Zener model (see Figure 2) provides a representation of the equilibrium state. This part can be modeled by any of the hyperelasticity-based classical models. Following Bergström [38], the Arruda-Boyce eight-chain model was selected. In the case of a unidirectional test, the stress-strain relationship can be expressed by [31]:

$$\sigma_{True}^{(R_1)} = C^{(R_1)}\left(\lambda^2 - \frac{1}{\lambda}\right)\frac{\sqrt{N^{(R_1)}}}{\lambda^{(R_1)}_{chain}} L^{-1}\left(\frac{\lambda^{(R_1)}_{chain}}{\sqrt{N^{(R_1)}}}\right) \quad (4)$$

With

$$\lambda^{(R_1)}_{chain} = \sqrt{\frac{\left(\lambda^2 + 2/\lambda\right)}{3}} \quad (5)$$

$$C^{(R_1)} = \frac{nK_BT}{3} \quad (6)$$

$$N^{(R_1)} = \frac{1}{3}\left[\lambda_{lim}^2 + \frac{2}{\lambda_{lim}}\right] \quad (7)$$

Where $\sigma^{(R_1)}$ is the true stress of the membrane in the equilibrium state given, λ is the extension ratio, λ_{lim} is the limit network stretch and L is the Langevin function defined by L(x) = coth(x) - 1/x. The engineering stress is related to the true stress by Equation (8).

$$\sigma_{True} = \lambda \sigma_{Eng} \quad (8)$$

The relationship between the spring modulus, the stress and the strain is given by Equation (9).

$$\sigma_{Eng} = E \varepsilon \quad (9)$$

Combining Equations (4) and (9) provides the modulus of the spring R_1.

$$E^{(R_1)} = \frac{C^{(R_1)} \left(\lambda - \frac{1}{\lambda^2} \right) \frac{\sqrt{N^{(R_1)}}}{\lambda^{(R_1)}_{chain}} L^{-1} \left(\frac{\lambda^{(R_1)}_{chain}}{\sqrt{N^{(R_1)}}} \right)}{\varepsilon} \quad (10)$$

Knowing the relation between the strain and the extension,

$$\varepsilon = \lambda - 1 \quad (11)$$

The final expression for the modulus of the spring R_1 can be obtained:

$$E^{(R_1)} = \frac{C^{(R_1)} \left(\lambda - \frac{1}{\lambda^2} \right) \frac{\sqrt{N^{(R_1)}}}{\lambda^{(R_1)}_{chain}} L^{-1} \left(\frac{\lambda^{(R_1)}_{chain}}{\sqrt{N^{(R_1)}}} \right)}{\lambda - 1} \quad (12)$$

As can be seen in Equation (12), the modulus of the spring R_1 is defined by two parameters. The first one, $C^{(R_1)}$, which is provided by Equation (6), is related to the shear modulus of the network in the equilibrium state. The second parameter is $N^{(R_1)}$, defined in Equation (7), which can be associated with the stretch limit of the network. Both parameters are material constants.

3.2. Representation of the deviation from the equilibrium state

The time-dependence behavior which represents the deviation from the equilibrium state corresponds to part B of the Zener model (see Figure 2). The spring R_2 is characterized by a non-linear stress-strain behavior while the time dependence is provided by the damper. The modulus of the spring R_2 can be obtained using the same method as described in section 3.1 for the spring R_1:

$$E^{(R_2)} = \frac{C^{(R_2)} \left(\lambda^{(R_2)} - \frac{1}{\lambda^{(R_2)2}} \right) \frac{\sqrt{N^{(R_2)}}}{\lambda^{(R_2)}_{chain}} L^{-1} \left(\frac{\lambda^{(R_2)}_{chain}}{\sqrt{N^{(R_2)}}} \right)}{\lambda^{(R_2)} - 1} \quad (13)$$

where $C^{(R_2)}$ and $N^{(R_2)}$ are the two parameters defining the spring R_2 and $\lambda^{(R_2)}$ is the extension ratio relative to the spring R_2. For the damper viscosity η, we propose to use the simple relationship shown in Equation 14 to describe its variation with the strain rate ζ.

$$\eta = A Ln(\zeta) + B \quad (14)$$

where *A* and *B* are constants characterizing the damper.

4. Determination methods for the model constants

This section describes the methods that have been used to obtain the constants $C^{(R1)}$ and $N^{(R1)}$ for the spring R_1, $C^{(R_2)}$ and $N^{(R_2)}$ for the spring R_2, and *A* and *B* for the damper.

4.1. Determination of the constants relative to the equilibrium state contribution

The membrane equilibrium state is represented by the mechanical behavior of the spring R_1. The spring modulus depends on two parameters, $C^{(R1)}$ and $N^{(R1)}$, according to Equation (12). $N^{(R1)}$ is related to the limit network stretch λ_{lim} (Equation (7)). This limit stretch corresponds to the theoretical maximum extension that the elastomer molecular chains can reach in the liquid state. It can be determined from a tension test as shown in Figure 3. A theoretical stress-strain curve is fitted to the experimental data, and λ_{lim} is provided by its theoretical asymptotic limit at large extension.

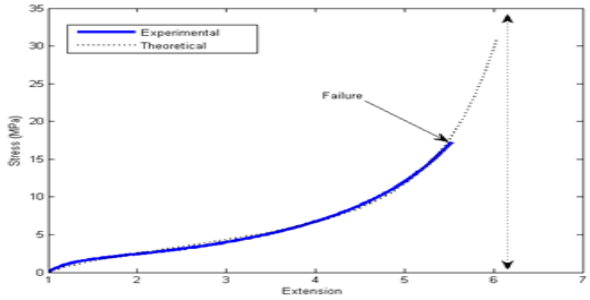

Figure 3: *Determination of the limit network stretch*

For its part, $C^{(R1)}$ is linked to the number of entanglements and the temperature (Equation (6)). It can be computed using the alternative expression provided by the Arruda-Boyce model [38]:

$$C^{(R_1)} = \frac{\sigma}{\left(\lambda - \frac{1}{\lambda^2} \right) \frac{\sqrt{N^{(R_1)}}}{\lambda^{(R_1)}_{chain}} L^{-1} \left(\frac{\lambda^{(R_1)}_{chain}}{\sqrt{N^{(R_1)}}} \right)} \quad (15)$$

Where $\lambda^{(R_1)}_{chain}$ et $N^{(R_1)}$ are given respectively by Equations (5) and (7). $C^{(R_1)}$ can be calculated for any location within the equilibrium state defined by a theoretical path laying between the sample loading and unloading curves as shown in Figure 4.

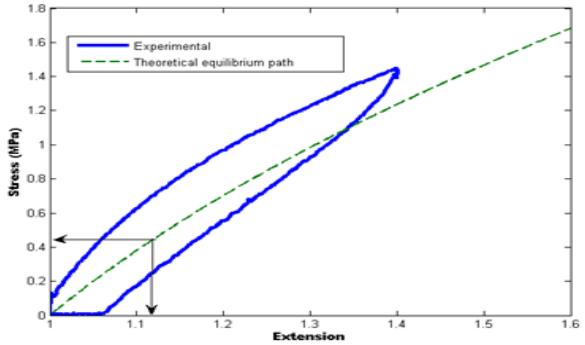

Figure 4: *Location of the theoretical equilibrium path relatively to the loading and unloading curves*

Since loading rates are comprised between 10 mm/min and 100 mm/min, an intermediate rate of 50 mm/min was selected for the determination of $C^{(R_1)}$.

4.2. Determination of the constants relative to the deviation from the equilibrium state

The contribution of the deviation from the equilibrium state to the elastomer behavior is essentially due to the part B of the model, i.e. the spring R_2 and the damper. In particular, these two components provide the time dependence of the system. The damper viscosity is provided in Equation 14. Here, the determination of the spring R_2 constants is shown.

4.2.1. Determination of the spring R_2 constants

The stress-strain expression for loading is provided by Equation (16), which is obtained from Equation 2 when $t < \tau_{1/2}$.

$$\sigma = \zeta\eta + E^{(R_1)}\varepsilon - \zeta\eta\, e^{-\frac{E^{(R_2)}}{\eta}\frac{\varepsilon}{\zeta}} \tag{16}$$

When ε is much smaller than 1, the slope of the curve representing Equation (16) is given by:

$$\lim_{x\to 0}\left(\frac{\partial\sigma}{\partial\varepsilon}\right) = E^{(R_1)} + E^{(R_2)} \tag{17}$$

The physical meaning of this result can be interpreted as the fact that, at the beginning of the deformation, the system stress is only controlled by the two springs, with no contribution of the damper. This can be attributed to the fact that, when the deformation begins, the damper strain rate is equal to zero, leading to a zero stress. The stress at the beginning of the deformation is thus the result of the contribution of a system composed of the two springs in parallel. This leads the system modulus at the origin being provided by the sum of the two spring modulus. Let's call E_t this slope at the origin deduced from the experimental stress-strain curve measured with the elastomer membrane.

$$E_t = E^{(R_1)} + E^{(R_2)} \tag{18}$$

The expressions for $E^{(R_1)}$ and $E^{(R_2)}$ are provided by Equations (12) and (13) respectively. At the beginning of the system loading, the springs R_1 and R_2 have the same extension ratio λ, consequently $\lambda^{(R_1)}_{chain}$ and $\lambda^{(R_2)}_{chain}$ are equals according to Equation (5). In addition, we can consider also that these two springs have the same limit stretch λ_{lim}. Thus, according to Equation (7), $N^{(R_1)}$ is equal to $N^{(R_2)}$ and the expression of E_t can be reduced to:

$$E_t = \frac{\left(C^{(R_1)} + C^{(R_2)}\right)\cdot\left(\lambda - \frac{1}{\lambda^2}\right)\frac{\sqrt{N}}{\lambda_{chain}}L^{-1}\left(\frac{\lambda_{chain}}{\sqrt{N}}\right)}{\lambda - 1} \tag{19}$$

The inverse of the Langevin function can be approximated by:

$$L^{-1}\left(\frac{\lambda_{chain}}{\sqrt{N}}\right) = 3\frac{\lambda_{chain}}{\sqrt{N}} + \frac{9}{5}\left(\frac{\lambda_{chain}}{\sqrt{N}}\right)^3 + \frac{297}{175}\left(\frac{\lambda_{chain}}{\sqrt{N}}\right)^5 + \ldots \tag{20}$$

For $\lambda \approx 1$, Equation (20) can be reduced to:

$$L^{-1}\left(\frac{\lambda_{chain}}{\sqrt{N}}\right) \approx 3\frac{\lambda_{chain}}{\sqrt{N}} \tag{21}$$

Equation (19) thus becomes:

$$E_t = 3\left(C^{(R_1)} + C^{(R_2)}\right)\frac{\left(\lambda - \frac{1}{\lambda^2}\right)}{\lambda - 1} \tag{22}$$

$C^{(R_2)}$ is provided by Equation (23), where $C^{(R_1)}$ is deduced from the experimental data using Equation (15) and E_t can be obtained from the slope of the loading stress-strain curve at the origin.

$$C^{(R_2)} = \frac{E_t}{3}\left[\frac{\lambda^2 + \lambda + 1}{\lambda^2}\right]^{-1} - C^{(R_1)} \tag{23}$$

4.2.2. Determination of the damper viscosity

The damper viscosity is described by a linear function of the strain rate logarithm (Equation (14)). The values of the constants A and B are obtained by regression using the mean square method as shown in Figure 5.

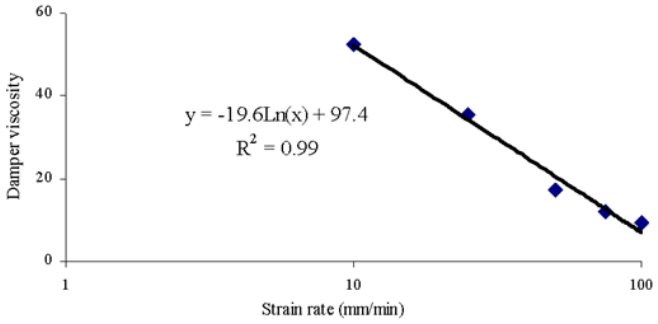

Figure 5: *Damper viscosity constants determination*

5. Results and Discussions

The measured loading-unloading stress-strain data represented in Figure 6 illustrate the non linear mechanical behavior of nitrile rubber. They also show the large effect of strain rate on the hysteresis loop corresponding to a cycle of loading-unloading.

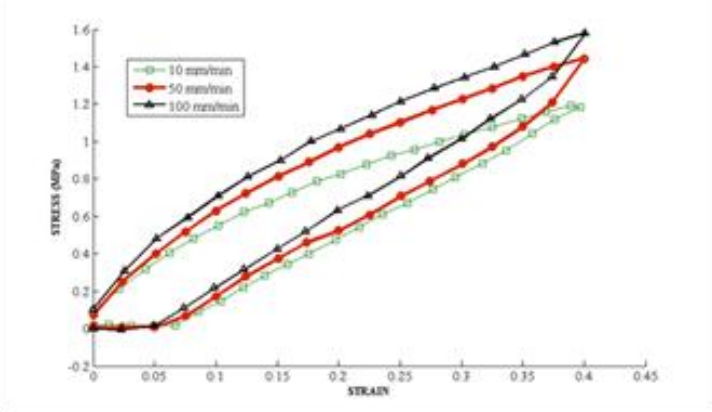

Figure 6: *Stress-strain behavior of nitrile rubber at different strain rates*

For a given strain rate, the hysteresis loop can be resolved into two curves as shown in Figure 7. The first one corresponds to the equilibrium state represented by the spring R_1. The second curve is associated with the deviation from this equilibrium state, described by part B of the Zener model (Figure 2).

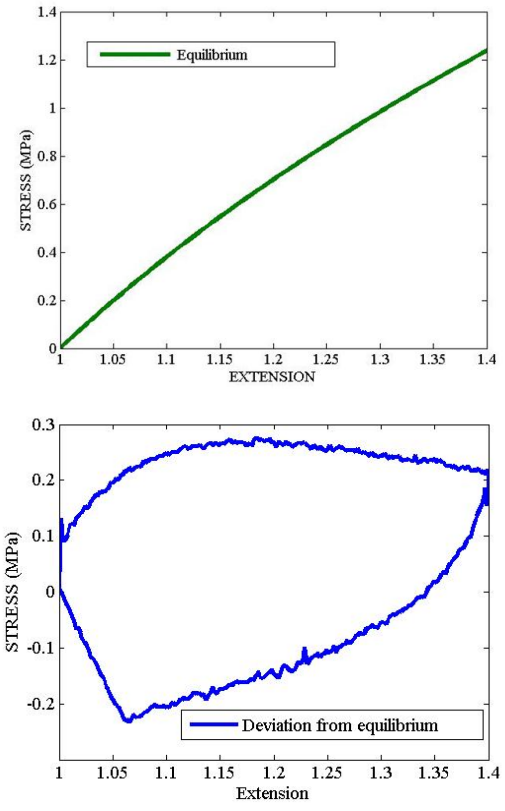

Figure 7: *Graphic decomposition of the stress-strain behavior of the rubber*

The values of the spring parameters used for the proposed description of the nitrile rubber hysteresis behavior, which should be valid at all strain rates, are determined from the test performed at 50 mm/min. They are provided in Table 1.

Table1: *Values of the spring parameters, obtained using 50 mm/min measurements*

	$C^{(R_1)}$ *(MPa)*	$C^{(R_2)}$ *(MPa)*	N
Spring R_1	0.46	*	370.54
Spring R_2	*	1.17	370.54

Figure 8 *displays the experimental results and those provided by the theoretical description using Table 1 parameter values for nitrile rubber hysteresis loop at 50 mm/min.*

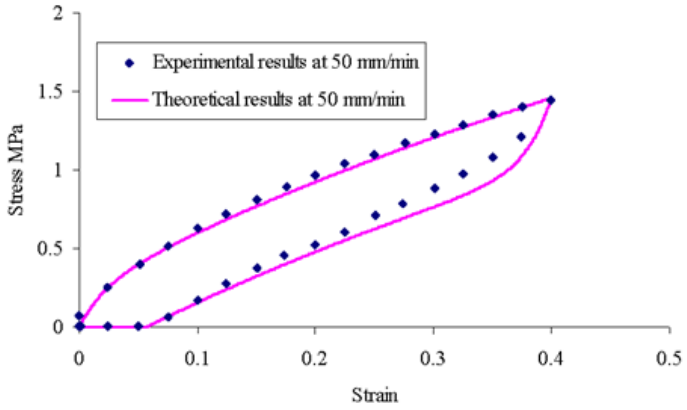

Figure 8: *Hysteresis stress-strain loop at 50mm/min for Nitrile rubber*

The values of the spring parameters obtained with the data measured at 50 mm/min were used to compute the nitrile rubber hysteresis stress-strain loop at others strain rates (10, 25, 75 and 100 mm/min). As shown in Figure 9, which displays the results obtained for strain rates of 10 and 100 mm/min, a relatively good correlation between experimental and theoretical results is obtained, especially for the loading part of the curve.

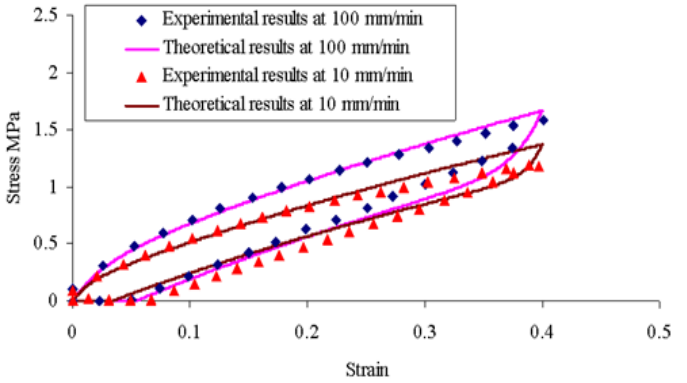

Figure 9: *Stress-strain behavior at 10 and 100 mm/min*

6 Conclusion

When they are used, protective gloves are subjected on a regular basis to cyclic deformations. In order to study the behaviour at large deformations and various strain rates of elastomers, which constitute a choice material for gloves, a model was developed based on a uniaxial loading-unloading configuration. The theoretical description was provided using Zener's rheological model in agreement with Bergström and Boyce's proposition that the elastomer behaviour is controlled by two contributions, the first one corresponding to the equilibrium state and the second one to a non-linear rate-dependent deviation from that equilibrium state. The validity of the description was verified with nitrile rubber samples. The parameters corresponding to the springs were obtained from measurements carried out at 50 mm/min. The damper viscosity is approximated by a linear function of the strain rate logarithm. A good agreement between the theoretical and experimental results was obtained. This simple description of the hysteresis behaviour of elastomers as a function of the strain rate provides a useful tool to estimate the mechanical behavior at various strain rates. Attempts will be made to extend this approach to the case of textiles and coated textiles, which are also used as protective glove materials.

Acknowledgment

This research has been supported by the Institut de recherche Robert-Sauvé en santé et sécurité du travail (IRSST). The authors would like to thank Professor Michel Beaudin for his mathematical advices.

References

[1]. Vu-Khanh, T., Dolez, P. I., Harrabi, L., Lara, J., Larivière, C., Tremblay, G., Nadeau, S., Caractérisation de la souplesse des gants de protection par des méthodes mécaniques et une méthode biomécanique basée sur l'électromyographie de surface. Étude et Recherche. 2007, Montréal: Institut de recherche Robert-Sauve´ en santé et en sécurité du travail au Québec. 90 pages.

[2]. Harrabi, L., Dolez, Patricia I., Vu-Khanh, Toan., Lara, Jaime., Evaluation of the flexibility of protective gloves. International Journal of Occupational Safety and Ergonomics. , 2008. 14(1): p. 61-68.

[3]. Harrabi, L., Dolez, Patricia I., Vu-Khanh, Toan., Lara, Jaime., Tremblay, Guy., Nadeau, Sylvie., Larivière, Christian., Characterization of protective gloves stiffness: Development of a multidirectional deformation test method. Safety Science, 2008. 46(7): p. 1025-1036.

[4]. Larivière, C., et al., Biomechanical assessment of gloves. A study of the sensitivity and reliability of electromyographic parameters used to measure the activation and fatigue of different forearm muscles. International Journal of Industrial Ergonomics, 2004. 34(2): p. 101-116.

[5]. Buhman, D.C., et al., Effects of glove, orientation, pressure, load, and handle on submaximal grasp force. International Journal of Industrial Ergonomics, 2000. 25(3): p. 247-256.

[6]. Betteni, F., Dispositivi di protezione individuale. Tinctoria, 2004: p. 37-43.

[7]. Gent, A.N., Engineering with rubber: How to design with rubber components. 2001, Munich: Hanser Publishers.

[8]. Kumar, A. and R.K. Gupta, Fundamentals of Polymer Engineering. 2 nd ed. 2003, New York: Marcel Dekker.

[9]. Mooney, M., A Theory of Large Elastic Deformation. Journal of Applied Physics, 1940. 11: p. 582-592.

[10]. Rivlin, R.S. Large Elastic Deformation of Isotropic Materials. Further development of the General Theory. in Phil. Trans. Roy. Soc. London. 1948.

[11]. Rivlin, R.S., Large Elastic Deformation of Isotropic Materials. Royal Society of London--Philosophical Transactions Series A, 1948. 241(835): p. 379-397.

[12]. Treloar, L.R.G., The Physics of Rubber Elasticity. 1975: Oxford University Press.

[13]. Treloar, L.R.G., Elasticity and related properties of rubbers. Rubber Chem. Technol, 1974. 47(3): p. 625-696.

[14]. Treloar, L.R.G., A non-gaussian theory for rubber in biaxial strain- I. Mechanical properties. Proc. R. Soc. London A, 1979. 369: p. 261-280.

[15]. Ogden, R.W., Large deformation isotropic elasticity- on the correlation of the theory and experiment for incompressible rubberlike solids. Proceedings of the Royal Society of London, Series A (Mathematical and Physical Sciences), 1972. 326(1567): p. 565-84.

[16]. Ogden, R.W., Background on nonlinear elasticity, Chapter 2.2, J. Lemaitre, Editor. 2001, in the handbook of materials behavior models: Boston. p. 75-83.

[17]. Yeoh, O.H., Some forms of the strain energy function for rubber. Rubber Chemistry and Technology, 1993. 66(5): p. 754-771.

[18]. Yeoh, O.H., Hyperelastic material models for finite element analysis of rubber. J. Nature Rubber Res., 1997. 12: p. 142-153.

[19]. Allen, G., et al., Thermodynamics of rubber elasticity at constant volume. Trans. Faraday Soc, 1971. 67: p. 1278-1292.

[20]. Allport, J.M. and A.J. Day, Statistical mechanics material model for the constitutive modelling of elastomeric compounds. Proceedings of the Institution of Mechanical Engineers, Part C: Journal of Mechanical Engineering Science, 1996. 210(6): p. 575-585.

[21]. Flory, P.J., Network structure and the elastic properties of vulcanized rubber. Chem. Rev., 1944. 35: p. 51-75.

[22]. Flory, P.J., Theory of elasticity of polymer networks. The effect of local constraints on junctions. J. Chem. Phys, 1977. 14(2): p. 80-92.

[23]. Ferry, J.D., Viscoelastic Properties of Polymers. 1980: John Wiley and Sons, Inc.

[24]. Gent, A.N. and thomas A.G., Forms of the stored (strain) energy function for vulcanized rubber. J. Polym. Sci, 1958. 28: p. 625-637.

[25]. Hart-Smith, L.J., Elasticity parameters for finite deformation of rubber-like materials. Z. Angew. Mathe. Phys., 1966. 17: p. 608-626.

[26]. Gumbrell, S.M., Mullins L., and Rivlin R.S., Departures of the elastic behaviour of Rubbers in simple extension from the kinetic theory. Trans Faraday Soc, 1953. 49: p. 1495-1505.

[27]. James, H.M. and Guth E., Theory of the elastic properties of rubber. J. Chem. Phys., 1943. 11(10): p. 455-481.

[28]. Mark, J.E., The constants 2 C_1 and 2 C_2 in phenomenological elasticity theory and their dependence on experimental variables. Rubber Chemistry and Technology, 1975. 48(3): p. 495-512.

[29]. Varga, O.H., Stress-Strain behavior of elastic materials: selected problems of large deformation. New York: Interscience publisher, 1966: p. 190 p.

[30]. Gee, G., The present status of the theory of rubber elasticity. Polymer., 1966. 7: p. 373-385.

[31]. Arruda, E.M. and M.C. Boyce, A three-dimensional constitutive model for the large stretch behavior of rubber elastic materials. Journal of the Mechanics and Physics of Solids, 1993. 41(2): p. 389-412.

[32]. Valanis, K.C. and R.F. Landel, Strain-energy function of hyperelastic material in terms of extension ratios. Journal of Applied Physics, 1967. 38(7): p. 2997-3002.

[33]. Von Lockette, P.R. and E.M. Arruda, A network description of the non-Gaussian stress-optic and Raman scattering responses of elastomer networks. Acta Mechanica, 1999. 134(1-2): p. 81-107.

[34]. McCrum, N.G., C.P. Buckley, and C.B. Bucknall, Principles of Polymer Engineering. 2004, New York: OXFORD UNIVERSITY PRESS.

[35]. Mullins, L., Softening of rubber by deformation. Rubber Chem. Technol, 1969. 42: p. 339-362

[36]. Kucherskii, A.M., Hysteresis losses in carbon-black-filled rubbers under small and large elongations. Polymer Testing, 2005. 24(6): p. 733-738.

[37]. Song, B., W. Chen, and M. Cheng, Novel model for uniaxial strain-rate-dependent stress-strain behavior of ethylene-propylene-diene monomer rubber in compression or tension. Journal of Applied Polymer Science, 2004. 92(3): p. 1553-1558.

[38]. Bergstrom, J.S. and M.C. Boyce, Constitutive modeling of the large strain time-dependent behavior of elastomers. Journal of the Mechanics and Physics of Solids, 1998. 46(5): p. 931-954.

[39]. Qi, H.J. and M.C. Boyce, Stress-strain behavior of thermoplastic polyurethanes. Mechanics of Materials, 2005. 37(8): p. 817-839.

[40]. ASTM D 412., Standard Test Methods for Vulcanized Rubber and Thermoplastic Elastomers - Tension. 1998, Annual Book of ASTM Standards

[41]. Doi, M. and S.F. Edwards, The Theory of Polymer Dynamics. 1986: Oxford University Press.

[42]. Bergstrom, J.S., Large Strain Time-Dependent Behavior of Elastomeric Materials, in Department of Mechanical Engineering. 1999, MASSACHUSETTS INSTITUTE OF TECHNOLOGY.